Stress–Strain Behavior and Tensile Dilatometry of Glass Bead-Filled Polypropylene and Polyamide 6

A. MEDDAD, B. FISA

Centre de Recherche Appliqué sur les Polymères (CRASP), École Polytechnique de Montréal, Montréal, Québec, H3C 3A7, Canada

Received 13 June 1996; accepted 5 August 1996

ABSTRACT: The mechanical behavior of multiphase materials is closely related to the interfacial adhesion between their various components. There is considerable interest in the development of simple experimental techniques for characterization of interfacial debonding during mechanical loading. Probably the best known method is tensile dilatometry, in which the onset and progression of debonding are related to the volume of microvoids generated in the material as it undergoes mechanical loading. Several authors have suggested that equivalent information can also be extracted from stress–strain data generated during a simple constant strain rate test. In practice, however, the transition between the initially well-bonded and the debonded state is obscured by the strain-induced softening of the matrix, which is usually observed in the same strain range as the debonding. In this work the filler/matrix debonding in polypropylene and polyamide 6 filled with up to 50 vol % of glass beads is examined using both tensile dilatometry and an analysis of tensile stress–strain curves. It was found that, depending on the level of adhesion, either a complete or partial debonding occurs in the strain range studied (0–8%). It appears that the volume change due to debonding is a small part of the total volume strain recorded. Therefore, the accuracy of the tensile dilatometry is not sufficient to detect the onset of debonding. The loss of stiffness of the composite, particularly when compared to the loss of stiffness of the matrix offers a more promising way to follow the debonding process. © 1997 John Wiley & Sons, Inc. J Appl Polym Sci **64:** 653–665, 1997

Key words: filler; polymer; debonding; dilatometry; stress–strain behavior

INTRODUCTION

The mechanical behavior of filled polymers and of other multiphase materials is closely related to the interfacial adhesion between their various components. When the adhesion is weak, the load-bearing capacity of the material is limited because phase separation occurs at low stress and strain. The development process of any filled plastic usually involves considerations related to the "compatibility" of the components. Filler particles surfaces are treated with adhesion promoters of various types. Conversely, the chemical structure of the polymer can also be tailored towards a better adhesion.

There is considerable interest in the development of simple experimental techniques that would make it possible to evaluate the efficiency of these treatments. Undoubtedly the most widely used method to measure the mechanical behavior of materials is the constant strain rate tensile test. Although the material properties generated by the short-term tensile test are only indirectly related to the in-use performance of polymer-based products, the test owes its widespread use to its great simplicity.

Constant strain rate methods have been evalu-

Correspondence to: Abderrahmane Meddad.
 CCC 0021-8995/97/040653-13

ated for the study of debonding. Vollenberg et al.[1] working with the glass bead-filled plastics, attributed a section of the stress–strain curve to the debonding process. Another method, conceptually more straightforward, consists of measuring the volume of the sample as it is being strained. The idea is that when the phase separation occurs, the material starts to dilate at a faster rate. The technique, tensile dilatometry, was recently reviewed by Naqui and Robinson.[2] It was applied by a number of workers to multiphase polymers materials. Bucknall et al.[3] have described one quantitative method based on the determination of the onset of phase separation and on the evaluation of the cavitation phenomenon. Pukánsky et al.,[4] using the dilatometry technique, have reported that in the polypropylene filled with calcium-carbonate particles, debonding initiation might coincide with the yielding point. Effect of silane treatment of beads was also evaluated by this technique.[5] It was reported that in the polyamide 6 filled with glass beads, the silane treatment tends to slow or to eliminate debonding phenomena. Working with glass bead filled polycarbonate, Heikens et al.[6] have proposed a method to obtain quantitative information on the determination of several possible deformation mechanisms from the total volume deformation.

The goal of this work was to evaluate and compare the tensile stress–axial strain curves and volume strain–axial strain curves of two model materials: glass bead-filled polypropylene and polyamide 6. In particular, we are interested in determining whether the stress and strain corresponding to the onset and development of interfacial separation can be determined from these curves. The experimental results presented here are used in a future article to model the kinetics of debonding during the tensile test.[7]

EXPERIMENTAL

Materials and Processing

The polypropylene used in this study was an injection grade resin, Profax 6301, from Himont Canada Ltd. The resin was in powder form with melt index of 12 g/10 min and a density of 0.91 g/cm^3. General purpose, unextracted polyamide 6, Zytel 211 (density 1.13 g/cm^3) from DuPont of Canada Inc. Glass beads (untreated and silane treated) having an average particle diameter of 45 μm and a density of 2.45 g/cm^3 were obtained from Potters Canada Ltd. Polypropylene/glass powder blends with different filler contents (5, 20, 40, 50 vol %) were molded on a Battenfield BA-C 750/300 injection press. The polyamide 6 formulations were first compounded on a twin screw extruder, then injection molded using concentrations of 0, 5, 25, and 40 vol %. The compounding and injection-molding conditions were those recommended by the resin suppliers. An experimental mold cavity, 3 mm deep, having the shape of the ASTM D638-type I tensile bar, was used to mold the samples.

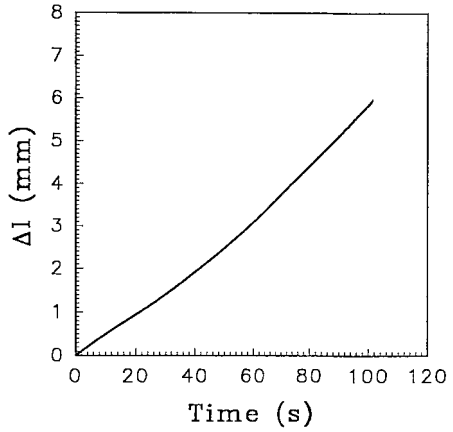

Figure 1 Typical axial strain Δl as recorded by the extensometer as a function of time (PP + 20 vol % untreated glass beads).

Mechanical Testing

A universal testing machine operating at the crosshead speed of 5 mm/min and a 2.5 kN maximum load was used. The strain data were collected using two extensometers; an MTS 638.13C axial extensometer (gage length 10 mm), and an Instron Model 6048.007 transverse extensometer (variable gage length) with 5 mm of maximum extension. These strains and stresses were recorded simultaneously using a data acquisition software at a frequency of 10 points per second during the tensile test. Figure 1 illustrates the use of the axial extensometer to determine the actual specimen strain rate. It can be observed that the actual gauge length of increase, Δl, recorded by the axial extensometer, as a function of time for 20 vol % filled polypropylene is nearly proportional to time and to crosshead displacement. The accuracy of the Instron extensometer is 5.7 μm and the MTS extensometer is accurate to 0.08% of 8%. The universal tensile machine is accurate to 1% of cell capacity used (1% of 5 kN

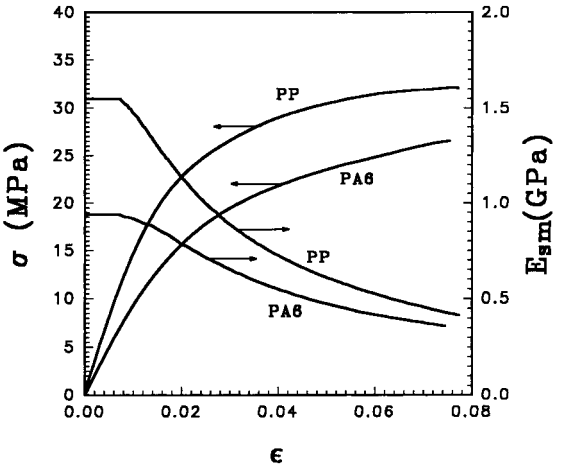

Figure 2 Stress σ and secant modulus E_{sm} of neat PP and neat PA6 as a function of axial strain ϵ.

in this case). From the stress–axial strain results, the behavior of the material can be represented by the nominal stress (σ) vs. nominal axial strain (ϵ) and the secant modulus E_s vs. ϵ can be extracted from the stress–axial strain results. Assuming that the transverse strain, ϵ_T, is identical in both directions perpendicular to the applied stress, the volume strain, ζ, is calculated using the following equation:

$$\zeta = (1 + \epsilon)(1 - \epsilon_T)^2 - 1. \qquad (1)$$

RESULTS AND DISCUSSION

Stress vs. Axial Strain Curves

Before considering the properties of filled systems, let us briefly describe the behavior of neat matrix resins. Figure 2 shows the stress vs. axial strain (σ vs. ϵ) and secant modulus vs. axial strain (E_{sm} vs. ϵ) curves of polypropylene and of polyamide 6. In the range of axial strains studied (0 to 8%) both materials first exhibit a constant stiffness zone (between 0 and 0.75%, approximately) with the initial modulus E_{0m} of about 1.57 GPa for polypropylene and of about 0.93 GPa for polyamide 6. In polypropylene, the breadth of this initial elastic zone is similar to that reported in the literature. Mariyama[8] also reported polypropylene to be elastic in strain range between 0 and 0.75%; the transition from the elastic to nonelastic behavior was interpreted in terms of strain softening due to the nonrecoverable deformation. With polypropylene, the constant stress plateau is reached at a strain of about 7.5% and at a stress of 32 MPa. Usually, by convention, this is considered as yield stress σ_y and yield strain ϵ_y (i.e., when $d\sigma/d\epsilon = 0$). Unfilled polyamide 6, on the other hand, does not reach a maximum. The "offset yield method," recommended by ASTM D-638M for this situation, gives a value of yield stress $\sigma_y = 18$ MPa and of yield strain $\epsilon_y = 2.7\%$. Using different conventions to determine the yield properties of these materials would make comparisons between them difficult. For this reason, for the purpose of this work we will compare, the state of both polymers (filled and unfilled) at a given constant strain of $\epsilon = 7.5\%$. The stress borne by the material at $\epsilon = 7.5\%$ is hereafter referred to as σ_s. For neat polyamide 6, $\sigma_s = 26.5$ MPa.

Figure 3 shows the stress–strain curves of polypropylene filled with glass beads. In Table I, the average values of several properties determined from the σ vs. ϵ curves are listed: the initial modulus, E_{0c}; the stress σ_0 and strain ϵ_0 at which the stress–strain curve deviates from linearity; the stress and the strain at yield, σ_y and ϵ_y (determined at $d\sigma/d\epsilon = 0$); and the stress at $\epsilon = 7.5\%$, σ_s. The principal points of the experimental results are:

1. All materials exhibit an elastic zone; the initial modulus E_{0c} increases with the filler content but is independent of the surface treatment.
2. The yield stress σ_y decreases with increasing filler content: σ vs. ϵ curves of all com-

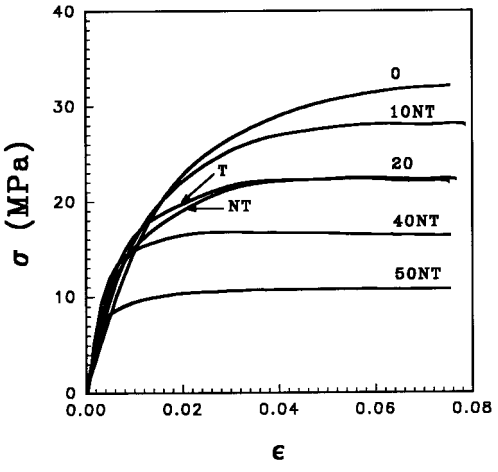

Figure 3 Stress σ vs. axial strain ϵ curves of filled PP. Numbers on curves denote glass concentration (vol %). The difference between treated (T) and untreated (NT) beads is shown for 20 vol % glass content.

Table I Summary of Tensile Properties of Glass Bead-Filled Polypropylene

Glass Content (vol %)	E_0 (GPa)	ϵ_0 (%)	σ_0 (MPa)	ϵ_y (%)	σ_y (MPa)	σ_g^* (MPa) Measured	σ_g^* (MPa) Calculated eq. (6)
0	1.57	0.75	11.9	7	32	—	—
5NT	1.8	0.53	9.5	6	30	31	30
5T	1.8	0.60	11.0	6	30	31	30
10NT	2	0.43	8.6	6	28	29	28
10T	2.1	0.51	10.5	4	28	29	28
20NT	2.4	0.30	7.3	4	22	23	22
20T	2.4	0.37	9.0	4	22	23	22
40NT	3.1	0.19	6.0	4	17	14	16
40T	3.2	0.25	7.9	3	18	14	16
50NT	3.8	0.13	5.3	2	10	11	10
50T	4.3	0.18	7.7	3	11	11	11

T = treated beads.
* $\epsilon = 7.5\%$.

posites fall below that of neat well before yield (in filled polypropylene, the yield stress and the stress at $\epsilon = 7.5\%$, σ_s are nearly identical).

3. Both the stress and the strain at which the material ceases to be elastic (σ_0 and ϵ_0) decrease with increasing filler content. The values of σ_0 and of ϵ_0 are higher with treated beads.
4. Although the transition between the linear (elastic) stage and the constant stress plateau starts at a higher strain with treated beads (T), the values of stress at $\epsilon = 7.5\%$, σ_s are identical for a given glass content (see, e.g., curves for the filler volume fraction $\phi = 0.2$, Fig. 3).

Filled polyamide 6 also has a linear zone at small strains and the initial modulus is unaffected by the surface treatment. Besides these similarities, there are significant differences between filled polypropylene and polyamide 6 filled with untreated beads, on the one hand, and polyamide 6 filled with treated beads (Fig. 4 and Table II). With untreated beads, the curves fall below that of neat polyamide 6 but at higher strains than in filled polypropylene. The departure from linearity in untreated glass–polyamide 6 composites follows a similar pattern as in filled polypropylene, i.e., the strain ϵ_0 decreases with increasing glass concentration. However, the stress σ_0 increases slowly with filler content. With treated glass, the strain ϵ_0 appears to be independent of the filler content. In fact, it is very close to the ϵ_0 value of the neat polyamide 6. The stress σ_0 increases substantially with the treated glass content. The stress–strain curves of polyamide 6 composites containing treated beads remain above the neat polyamide 6 curve. For a given glass concentration, the curves, nearly identical at small strains, diverge as the composite containing untreated beads starts to yield. The yield stress and strain (σ_y and ϵ_y, determined by the "offset yield method") decrease with increasing concentration of untreated beads. With treated beads, both the yield stress (σ_y) and the stress at $\epsilon = 7.5\%$ (σ_s)

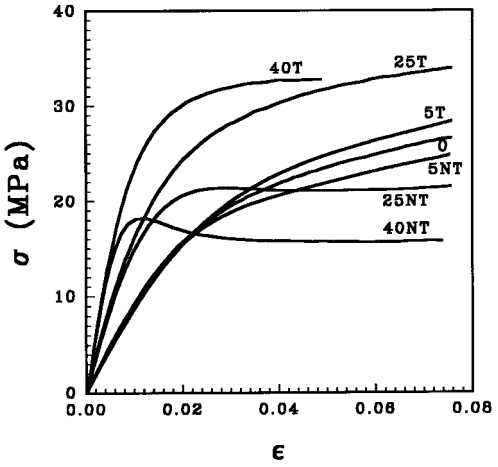

Figure 4 Stress σ vs. axial strain ϵ curves of filled PA6. Numbers on curves denote glass concentration (vol %). T: treated, NT: untreated glass.

Table II Summary of Tensile Properties of Glass Bead-Filled PA6

Glass Content (vol %)	E_0 (GPa)	ϵ_0 (%)	σ_0 (MPa)	ϵ_y (%)	σ_y (MPa)	σ (MPa) Measured	σ (MPa) Calculated eq. (6)
0	0.92	0.73	6.8	2.7	18	—	—
5NT	0.98	0.63	6.50	2.5	17	25	24
5T	1.05	0.71	7.4	1.5	13	28	24
25NT	1.9	0.40	7.3	2.3	21	21	16
25T	1.9	0.71	13.6	1.20	18	34	16
40NT	2.8	0.32	9.4	1	18	16	12
40T	3.0	0.65	19.7	1.1	34	33*	12

T = treated beads.
* ϵ = 4.5%.

increase with the glass content. The composite with the highest treated filler content (40 vol %) broke at a relatively low axial strain of about 4.5%.

We will now attempt to interpret the stress–strain behavior of these filled polymers. There are many equations relating the composite and the matrix stiffness. For a material containing spherical inclusions, one of the better known and widely used is the Kerner–Lewis equation[9]:

$$E_c = E_m \frac{1 + A_1 B_1 \phi}{1 - B_1 \Psi \phi} . \quad (2)$$

The constant A_1 is determined by the matrix Poisson ratio:

$$A_1 = \frac{7 - 5\nu}{8 - 10\nu} . \quad (3)$$

The other constant, B_1, accounts for the relative modulus of filler and of the matrix:

$$B_1 = \frac{\frac{E_f}{E_m} - 1}{\frac{E_f}{E_m} + A_1} \quad (4)$$

with E_f and E_m representing the filler and the matrix moduli, respectively.

The factor Ψ is a "crowding factor":

$$\Psi = 1 + \phi \left(\frac{1 - \phi_m}{\phi_m^2} \right) \quad (5)$$

with ϕ_m corresponding to the maximum filler volume packing fraction.

Use of the Kerner–Lewis equation is restricted to macroscopically homogeneous, isotropic bodies that are composed of homogeneous isotropic phases. Further to that are assumed perfect adhesion, and the uniform distribution of the particles. All these considerations aim at a characterization of the behavior of the composite material by means of the properties of the individual phases, their geometry (shape and dimensions), distribution, and concentration.[9,10] The equations of this type have been successfully applied to a broad variety of materials including those containing more than one dispersed phase and foams. In this last case the Kerner–Lewis equation becomes (assuming $E_f = 0$):

$$E_c = E_m \frac{1 - \phi}{1 - B_2 \Psi \phi} \quad (6)$$

where $(B_2) = -1/A_1$. Using the values of the matrix initial modulus E_{0m} = 1.57 GPa as E_m, its initial Poisson ratio ν_0 = 0.39 as ν, and the book value of 72 GPa of glass elastic modulus as E_f, and taking ϕ_m = 0.64, the Kerner–Lewis equation yields the E_{0c} vs. ϕ dependence shown in Figure 5 (full line). The agreement with the experimental values of initial modulus E_{0c} is fair except at high filler content (ϕ = 0.4 and ϕ = 0.5). The discrepancy between the measured and the calculated initial moduli at higher filler content is usually attributed to the fact that the material no longer satisfies the assumptions employed in the development of the Kerner–Lewis equation. The model does not take into account particle size nonunifor-

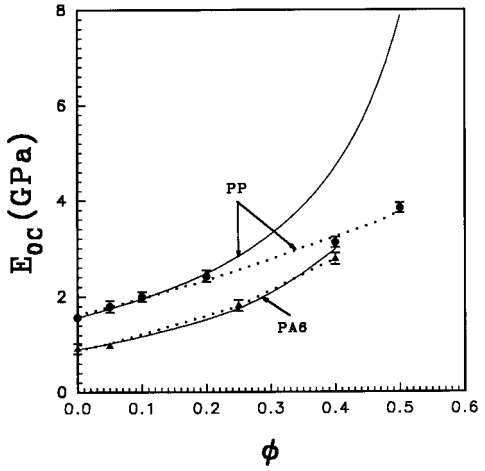

Figure 5 Initial modulus ($\epsilon \sim 0$) E_{0c} as a function of filler volume fraction ϕ. Points indicate experimental results, full lines were calculated from eq. (2) using constants of the second column—Table III; dotted lines ($\cdots$) using: "fitted" constants (third column—Table III).

mity, degree of aggregation, and the lateral restraint at high degrees of filling.[9–11]

One can also consider the Kerner–Lewis equation as a simple interpolation formula and determine the values of its constants that fit the experimental data. The curve-fitting procedure yields constants shown in Table III. These values differ slightly from those based on the filler and the matrix properties but a good fit with the experimental results for all filler concentrations is obtained even when a constant value of Ψ is assumed (dotted line Fig. 5).

The behavior of filled polypropylene appears to be relatively simple to interpret. At small strains it behaves as well-bonded composite. The constant value of the secant modulus is an indication that no debonding or other damage occurs below ϵ_0. Because, at small strains, the stress–strain curves of treated and untreated composites coincide and the values of σ_0 and ϵ_0 are lower than those of the neat resin, the point when the stress–strain curve starts to deviate from linearity can be attributed to the onset of debonding. In filled polymers, the stress corresponding to the onset of debonding consists of two principal contributions.[1] The first one is due to the adhesion at the filler–matrix interface. In practice, this adhesion stress is varied by the use of adhesion promoters (silanes, titanates, etc.) or inhibitors (e.g., silicone oil, refs. 5 and 12). The other is the thermal compression stress, which results from higher thermal expansion coefficient of the matrix compared to that of the filler. This causes the matrix to shrink around the filler particles as the material is being cooled from the melt temperature to the service temperature. This thermal stress has to be overcome when the filled polymer is subjected to an externally applied stress. Obviously, the magnitude of the thermal stress depends among other parameters on the thermal expansion coefficient differential between the filler and the surrounding material.[1,13] With a higher filler content this differential is smaller (because the "surrounding material" consists of the filler and the matrix). Therefore, the thermal stress should decrease with the increasing filler concentration, and with other things being equal, the debonding starts at a lower applied stress in more highly filled materials.

The effect of the coupling agent on ϵ_0 and σ_0 is relatively small, but significant. As the data in the Table I indicate, the values of σ_0 in treated bead composites are higher by about 2 MPa than in materials containing untreated beads. The stress–strain curves coincide again at yield. This suggests that regardless of the surface treatment, a completely debonded state has been reached. The Kerner–Lewis equation can again be applied. Using the value of the matrix secant modulus at $\epsilon = 7.5\%$ as E_m (0.47 GPa), the Kerner–Lewis equation can be used to calculate the stresses borne by the fully bonded [eq. (2)] or by the completely debonded [eq. (6)] composite, assuming the debonded composite behaves as a foam containing volume fraction of voids equal to ϕ. The agreement between the experimentally deter-

Table III Parameters Used to Calculate the Initial Composite Modulus E_{0c} from eq. (1) Based on the Component Properties (First Column) and Those Determined by Curve Fitting From E_{0c} vs. ϕ Curve (Untreated Bead Composites)

Material		Constituents	Curve Fitting
PP	E_m (GPa)	1.57	1.62
	A_1	1.23	1.68
	B_1	0.95	0.85
	ψ	$1 + 0.88\phi$	0.60
PA6	E_m (GPa)	0.92	0.88
	A_1	1.40	1.90
	B_1	0.97	1.03
	ψ	$1 + 0.88\phi$	1.04

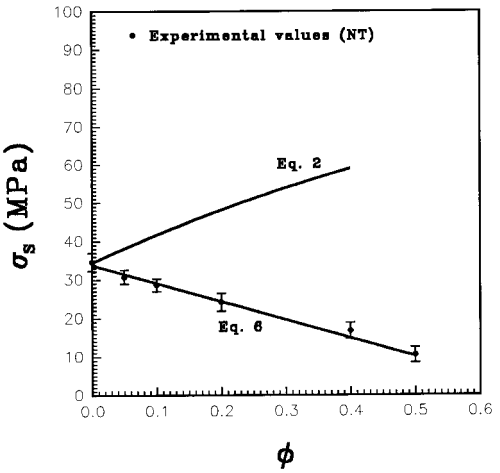

Figure 6 Stress at $\epsilon = 7.5\%$, σ_s of filled PP vs. filler volume fraction ϕ. Points indicate experimental results, full lines were calculated from eqs. (2) and (6) using "fitted" constants (third column—Table III).

mined values of σ_s and those calculated with the help of eq. (6) is excellent (Fig. 6).

The behavior of filled polyamide 6 can be analyzed using the same approach. The initial modulus calculated using the Kerner–Lewis equation is in good agreement with the experimental data and the "fitted" values of parameters (A_1, B_1, and Ψ) differ only slightly from those calculated using the component properties (Fig. 5 and Table III). Considering the polar nature of polyamide 6 when compared to polypropylene, it is reasonable to expect that there will be a higher degree of adhesion at the glass–polymer interface. Because, with untreated glass, the composites again deviate from the linearity at strains when the matrix is still elastic, the loss of elasticity at ϵ_0 can be attributed to the onset of debonding. The fact that the σ_0 increases slightly with the filler concentration underlines the difference between the applied stress (σ) and the local stress at the filler–matrix interface. To the applied debonding stress corresponds a local stress affected by the stress concentration at the interface. The stress concentration effect is determined by the stiffness differential between the particle and the surrounding material. With a higher filler concentration this differential is smaller and, at a given value of applied stress, the local stress will be lower leading to a lower probability of debonding. With treated glass–polyamide 6 composites the stress–strain curves remain well above that of the neat resin. In addition, the strain ϵ_0 appears to be independent of the filler content. It is, therefore, unclear at this stage if any debonding occurs in the treated bead polyamide 6 in the range of strains considered.

Using the Kerner–Lewis equation to calculate the stress borne by the composite at $\epsilon = 7.5\%$ gives results shown in Figure 7. In this case, the experimental results are between those predicted by eqs. (2) and (6). Considering that in filled polypropylene the stress σ_s calculated with the help of eq. (6) corresponds to that determined experimentally, the fact that in filled polyamide 6 the experimental values of σ_s are considerably higher even with untreated glass strongly suggests that, unlike in polypropylene, the debonding is not complete at $\epsilon = 7.5\%$.

The degree of interface adhesion in multiphase materials is often evaluated from the micrographs of fractured surfaces. The typical results of this type of analysis are shown in Figure 8(a) and (b). Samples containing 5 vol % of beads were deformed to an axial strain $\epsilon = 7\%$, broken in liquid nitrogen, and observed in scanning electron microscope. The matrix debonded from untreated beads creating elongated cavities [Fig. 8(b)], while the treated beads appear to remain solidly anchored to the matrix [Fig. 8(a)]. While the fractured surface of Figure 8(a) and (b) represent a kind of median (or most frequently observed) situation for each type of bead, they do not provide a completely accurate description of the material. In fact, it is possible to find in untreated glass–polyamide 6 composites a significant proportion of filler particles that have not separated from the

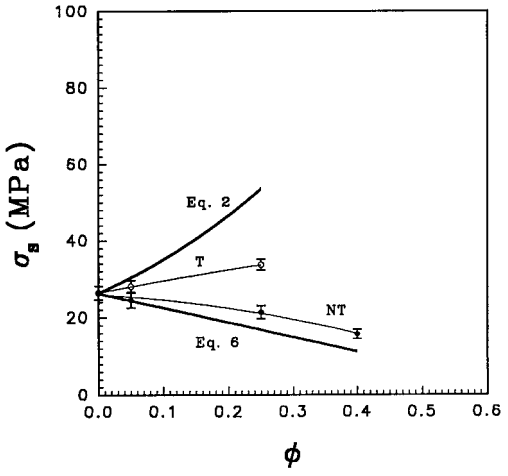

Figure 7 Stress at $\epsilon = 7.5\%$, σ_s of filled PA6 vs. filler volume fraction ϕ. Points indicate experimental results, full lines those calculated from eqs. (2) and (6) using "fitted" constants (third column—Table III).

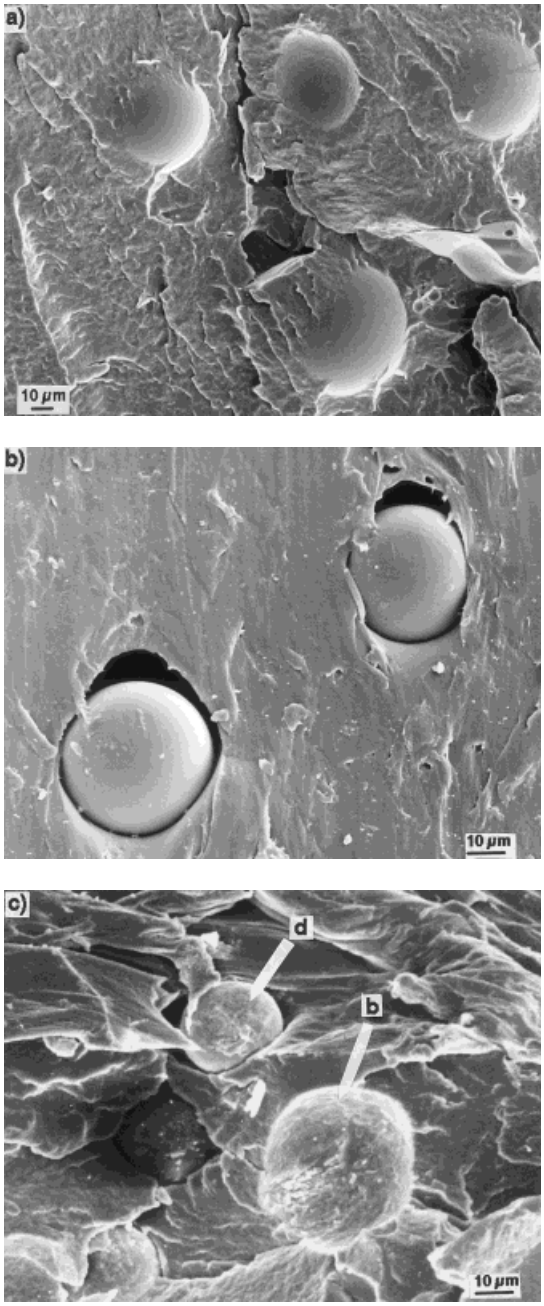

Figure 8 SEM pictures of PA6 + 25 vol % glass beads samples strained to $\epsilon = 7\%$ and broken at liquid N_2 temperature. (a) Silane-treated glass. (b) and (c) Untreated glass (arrows indicate (d) debonded bead and (b) bonded bead).

matrix [Fig. 8(c)]. Conversely, in treated bead composites a significant number of debonded particles have been observed at this strain.

In summary, the stress–strain curves indicate the onset of debonding when the linear elastic zone is shorter than that of the matrix. When the Kerner–Lewis equation is used to calculate the stress borne by the fully debonded polypropylene glass composite assuming it behaves as a foam, excellent agreement with experimental results is obtained. With polyamide 6 glass composite, the experimentally determined values are higher than those calculated from eq. (6). This suggests that the debonding is incomplete. Results obtained by scanning electron microscopic confirm the validity of this hypothesis.

Tensile Dilatometry

Figure 9 shows the volume strain versus axial strain (ζ vs. ϵ) curves of polypropylene containing 0 and 20 vol % of glass beads. The neat ζ vs. ϵ polypropylene curve starts to deviate from linearity at about the same strain as the tensile stress–axial strain curve. Above ϵ_0, the volume strain is smaller than that calculated from eq. (1) using the initial value of Poisson ratio $\nu_{0m} = 0.37$ and taking $\epsilon_T = \nu_{0m} \cdot \epsilon$ (dotted line). For example, at $\epsilon = 7.5\%$ eq. (1) predicts the volume strain $\zeta = 1.6\%$, while the experimental value is equal to 1.2%. The onset, at ϵ_0, of stress-induced viscoelastic reorganization of material is therefore detectable both from the σ vs. ϵ and ζ vs. ϵ curves.

The curves of filled polypropylene exhibit two linear parts: the first one being determined by the initial Poisson ratio, ν_{0c}, which, for $\phi = 0.20$, is equal to 0.3. This value is in agreement with that predicted by the Chow equation[14]:

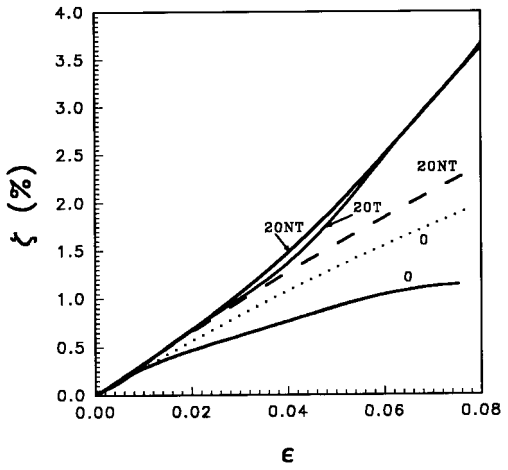

Figure 9 Volume strain ζ vs. axial strain ϵ of neat PP and of PP-filled with 20 vol % glass beads (T: treated; (NT): untreated glass. Dotted line (· · · ·) indicates dilational behavior of filled PP.

Table IV Summary of the Tensile Dilatometry Results on Glass Bead-Filled Polypropylene

Glass Content (vol %)	Initial Poisson Ratio ν_0	Slope of ζ vs. ϵ Curve at $\epsilon > \epsilon_y$	ζ (%) Measured at $\epsilon = 7.5\%$	ζ (%)[a] at $\epsilon = 7.5\%$ Calculated
0	0.37	0.06	1.2	1.6
5NT	0.36	0.56	2.0	1.8
5T	0.36	0.56	2.0	1.8
10NT	0.33	0.60	2.7	2.2
10T	0.33	0.60	2.7	2.2
20NT	0.30	0.68	3.3	2.7
20T	0.30	0.68	3.3	2.7
40NT	0.29	0.75	5.0	2.8
40T	0.29	0.72	4.8	2.8
50NT	0.27	0.80	6.0	3.2
50T	0.27	0.77	4.7	3.2

T = treated beads.
[a] Using eq. (1) and assuming $\epsilon_T = \nu_0 \cdot \epsilon$.

$$\frac{1 - 2\nu_{0c}\phi}{E_{0c}} = \frac{1 - 2\nu_{0m}}{\left[1 + \dfrac{\phi}{\gamma(1 - \phi)}\right] E_{0m}} \tag{7}$$

where E_{0c}, ν_{0c}, E_{0m}, and ν_{0m} are the initial modulus and Poisson ratio of composite and matrix, respectively. The coefficient γ is defined as follows:

$$\gamma = \frac{1 - \nu_{0m}}{3(1 - \nu_{0m})}. \tag{8}$$

The initial slope of the ζ vs. ϵ curve is independent of the filler treatment. The curve then turns upwards (at $\epsilon \approx 2\%$ for $\phi = 0.2$) before becoming linear again; the slope of the second stage is significantly higher than that of the first one.

In the transition stage (between strains of 2 to 6% for $\phi = 0.2$), the ζ vs. ϵ curve of the untreated composite remains slightly above that of its untreated counterpart. It is also worth noting that the curves of the filled polymers start to diverge from that of the matrix at strains below 1%. Results of ζ vs. ϵ tests on filled polypropylene are summarized in Table IV.

The volume strain vs. axial strain curves of neat and filled polyamide 6 ($\phi = 0.25$) are shown in Figure 10. For other filled polyamide 6 compositions results are summarized in Table V. The behavior of neat polyamide 6 is similar to that of polypropylene. During the first elastic stage, which is observed at $\epsilon < 0.74\%$, the Poisson ratio is 0.46. It is worth noting that between 2 and 5% axial strain the polyamide 6 volume is nearly constant. Above 5% the volume starts increasing at a faster rate. At small strains, the ζ vs. ϵ curves of polyamide 6, filled with treated or untreated glass coincide up to $\epsilon \approx 1.5\%$ (for $\phi = 0.25$). The curves then diverge, the volume of untreated glass composite increases at a much higher rate than that of treated glass. At $\epsilon = 7.5\%$, the volume strain recorded with untreated glass-filled polyamide 6 is 2.3% compared to 1.0% obtained with treated glass. Both untreated and treated glass-filled polyamide 6 values are significantly higher than those calculated using the low strain values of composite Poisson ratio.

When one attempts to relate the ζ vs. ϵ curves to the debonding process using the approaches

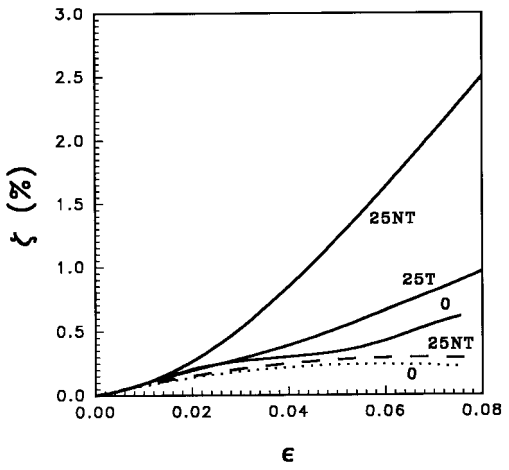

Figure 10 Volume strain ζ vs. strain ϵ of neat PA6 and of PA6-filled with 25 vol % glass beads. (T): treated; (NT): untreated glass. Dotted line (· · · ·) indicates dilational behavior of filled PA6.

Table V Summary of Tensile Dilatometry Results on Glass Bead-Filled Polyamide 6

Glass Content (vol %)	Initial Poisson Ratio ν_0	Slope of the ζ vs. ϵ Curve at $\epsilon > \epsilon_y$	ζ (%) Measured at $\epsilon = 7.5\%$	ζ (%)[a] at $\epsilon = 7.5\%$ Calculated
0	0.46	0.04	0.7	0.21
5NT	0.45	0.15	0.9	0.36
5T	0.45	0.10	0.8	0.36
25NT	0.44	0.45	2.3	0.52
25T	0.44	0.15	1.0	0.52
40NT	0.42	0.61	4.0	0.83
40T	0.43	0.22	1.2	0.67

T = treated bead.
[a] Using equation 1 and assuming $\epsilon_T = \nu_0 \cdot \epsilon$.

outlined in the literature different results are obtained with each approach. For example, the hypothesis that debonding initiation coincides with the intersection of the two linear stages of the ζ vs. ϵ curve was examined in ref. 4. In polypropylene filled with 20% vol % of glass, this intersection is situated at an axial strain of about 4%. Acceptance of this hypothesis would make the debonding initiation coincide with the yield of the filled polymer. At yield ($\epsilon_y = 4.2\%$, $\sigma_y = 22$ MPa, $\phi = 0.2$ of untreated glass) the stress borne by the composite is significantly lower than that measured on neat polypropylene at the same strain; therefore, the load-bearing section of the composite must have already been greatly reduced by the phase separation process. It is clear that the debonding started at a lower strain.

Another approach suggests that the point when the experimental ζ vs. curve deviates from the dilational behavior corresponds to the onset of debonding. Again, using the 20 vol % untreated glass/polypropylene composite as an example, this occurs at an axial strain of about 2% (see Fig. 9). However, the matrix itself deviates from dilational behavior already at $\epsilon = 0.75\%$. Therefore, the observed linearity of the ζ vs. ϵ function below $\epsilon = 2\%$ is probably coincidental: the additional void volume due to debonding of the glass–polypropylene interface compensates for the deviatoric behavior of the matrix. This method, therefore, also appears to overestimate the stress and strain at which the filler–matrix separation is initiated. With other glass concentrations, both in polypropylene and in polyamide 6, the Naqui and Robinson approach[2] yields similar results (see the last column of Tables IV and V and Fig. 11, curves 1–2, and Fig. 12, curves 1–3 and 2–3). The experimentally determined values of volume strain are always higher than those calculated from eq. (1) using the low strain value of Poisson ratio. This indicates that at least some cavitation must have occurred. However, the real volume strain due to cavitation must be, in this case, greater than the difference between the measured volume strain of the composite and that calculated from eq. (1) by a factor that would take into account the deviatoric behavior of the matrix.

According to Sinien et al.[12] the cavitational volume can be determined by substracting the matrix volume strain from the volume strain of the composite. The cavitation volume calculated using this method is shown in Figures 11 (polypropylene, curve 1-3) and 12 (polyamide 6, curves 1-4 and 2-4). The results for polypropylene show that in the range of strains where the debonding occurs (0.3 to 1.5%, $\phi = 0.2$), the volume generated is very small and is of the same order of

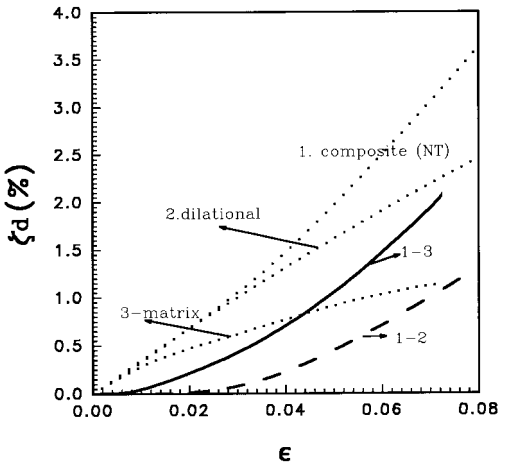

Figure 11 Volume strain of the composite from which the dilational volume strain calculated from eq. (1) was substracted (curve 1–2) and from which the experimental matrix volume strain was substracted (curve 1–3). Filled PP ($\phi = 0.2$, untreated glass).

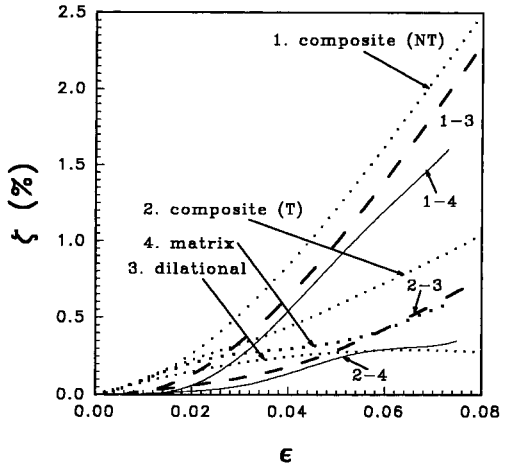

Figure 12 Volume strain of the composite from which the dilational volume strain calculated from eq. (1) was substracted (curve 1–2) and from which the experimental matrix volume strain was substracted (curve 1–3). Filled PA6 (ϕ = 0.25), treated (T), and untreated (NT) glass).

magnitude as the experimental error. This suggests that the debonding process does not generate a substantial volume strain until it is already well advanced. In addition, the slope of the post yield stage is not necessarily proportional to the filler content (see Fig. 13). In neat polypropylene, the postyield slope is only 0.06. It jumps to 0.56 for the lowest concentration of glass beads but a further rate of increase with ϕ is relatively slow. This shows that, following yield, phenomena other than an orderly elongation of a constant number of debonded ellipsoidal vacuoles play a role.

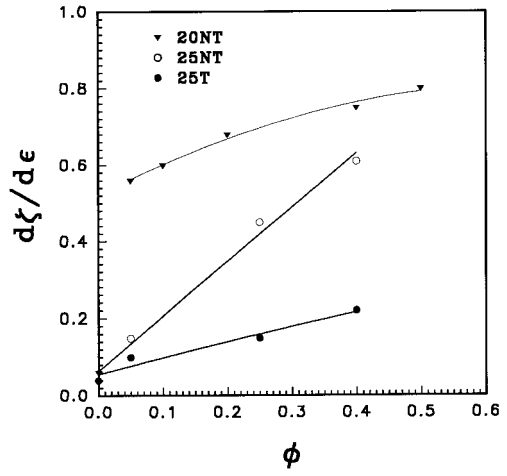

Figure 13 Postyield slope of the ζ vs. ϵ curves as a function of filler volume fraction ϕ.

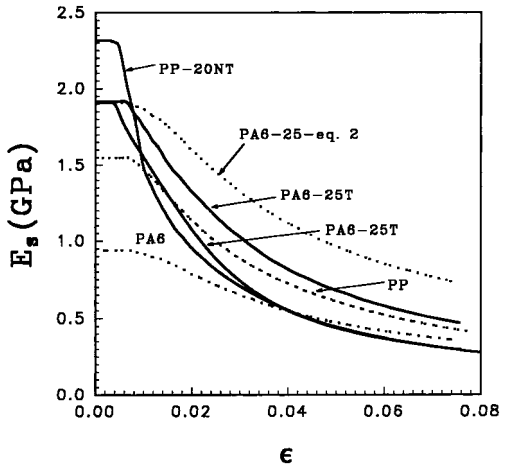

Figure 14 Secant modulus E_s of neat PP, PA6, and PP-filled with 20 vol % glass beads and PA6-filled with 25 vol % glass beads (T: treated and NT: untreated) as a function of axial strain ϵ.

As for filled polyamide 6, the results confirm that the debonding progresses at a rate slower than in filled polypropylene. With treated beads the cavitational volume is significant but smaller than both in untreated glass filled polyamide 6 or polypropylene. The incremental postyield slope in filled polyamide 6 (compared to neat polymer) is proportional to the filler content and is much larger when glass beads are not treated (Fig. 13). This is a further indication that with treated glass beads the debonding is not completed in the range of strains studied.

DISCUSSION

Although the concept of tensile dilatometry appears to offer a straightforward approach to detect and to monitor the debonding process, the results of this work show that in viscoelastic materials the results tend to be obscured by the deviatoric behavior of the matrix. Moreover, the volume strain due to debonding is small. Comparison of stress–axial strain (σ vs. ϵ) and volume strain–axial strain (ζ vs. ϵ) data suggests that the loss of stiffness during the constant strain rate tensile test can also be linked to the debonding process. Figure 14 shows the tensile secant modulus of neat and filled polypropylene (ϕ = 0.2, untreated glass) and of neat and filled polyamide 6 (ϕ = 0 and 0.25, treated and untreated glass) as a function of strain. As discussed above, wherever the composite modulus starts to decrease when the

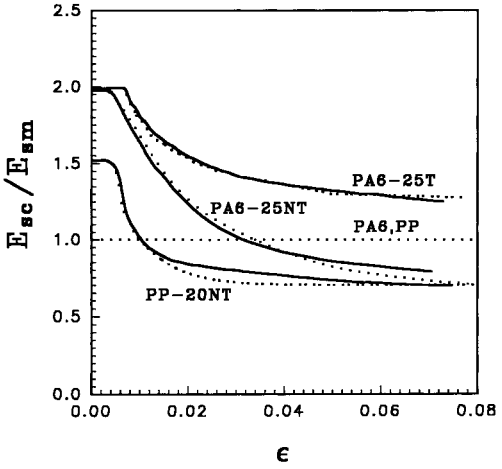

Figure 15 Secant moduli ratio E_{sc}/E_{sm} as a function of strain ϵ.

matrix is still elastic (polypropylene and polyamide 6 filled with untreated beads), the stress and strain at the end of the constant stiffness stage can be safely associated with the onset of debonding process.

The question of the onset of the debonding process (or of other damage) in treated glass–polyamide 6 composites merits further discussion. For this material both the dilatometry and the microscopy have shown a partial debonding at the strain $\epsilon = 7.5\%$. The initial rate of decrease (at $\epsilon > \epsilon_0$) exhibited by the secant modulus of the treated glass–polyamide 6 composite is very close to that of untreated glass counterpart (Fig. 14). The measured secant modulus of this composite is also significantly lower (at $\epsilon \geq \epsilon_0$) than that calculated from the Kerner–Lewis equation [eq. (2)] using the secant modulus of the matrix as E_m (see Fig. 14). The effect of matrix viscoelasticity can be reduced or possibly eliminated by plotting the ratio of the composite secant modulus and of the matrix secant modulus measured at the same strain. This is shown in Figure 15. Again, the initial rate of decrease of the E_{sc}/E_{sm} ratio at strains slightly above ϵ_0 are similar in treated and untreated glass–polyamide 6 composites.

Another strong evidence that in polyamide 6 treated glass composite the debonding starts at or near ϵ_0 was obtained from "load–unload" tests that were performed as follows: the specimen is first strained approximately to 0.5%, the test is then stopped, the sample is unloaded and allowed to relax for 30 min, and the procedure is repeated using the same sample except that the test is stopped at a higher strain. The initial modulus is determined for each cycle. The results of this load–unload test on the 25 vol % filled polyamide 6 are shown in Figure 16. For the neat polyamide 6, the modulus determined from the load–unload test is essentially constant in the same range of strains as that in standard tensile test. In untreated glass–polyamide 6 composite the constant stiffness zone is much smaller and the load–unload modulus drops rapidly below that of the neat matrix in a manner similar to the standard tensile test with the secant modulus. In polyamide 6 filled with treated glass, the modulus also decreases with prestrain ϵ_p but at a lower rate. In both cases, this is an indication that prestrained materials have undergone some damage from the point when the load–unload modulus starts to decrease.

CONCLUSION

The results of this work, carried out on two model systems, suggest that tensile dilatometry is not sufficiently sensitive for detection of the debonding process in viscoelastic polymers filled with glass beads. The debonding can be more easily related to the progressive loss of stiffness as the material undergoes straining. In polypropylene, the debonding is completed at yield point with untreated and silane treated glass. The Kerner–Lewis equation can be applied to calculate the yield stress of the fully debonded materials assuming its behavior is that of a foam. In filled polyamide 6, the adhesion at the filler–matrix in-

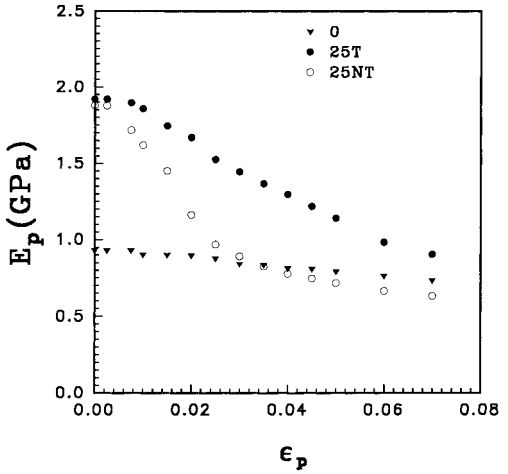

Figure 16 Initial modulus ($\epsilon \to 0$) determined from the load–unload test as a function of "prestrain" ϵ_p (filled PA6, $\phi = 0.25$).

terface is better, the debonding occurs at a slower rate, and is not complete when the material yields. In filled polypropylene and in polyamide 6 filled with untreated beads, the materials cease to be elastic where their respective matrices are still elastic. Therefore, the departure from elasticity corresponds to the onset of debonding. Polyamide 6 containing treated beads is elastic in the same range of strains as the neat polymer. However, the evaluation of the relative loss of stiffness expressed as the ratio of the composite and matrix secant moduli and the results of the load–unload test both strongly suggest that in this case the debonding initiation also coincides with the departure from elasticity. The ratio of the composite and matrix secant moduli, therefore, makes it possible to detect the onset of debonding and to evaluate its progression.

NOMENCLATURE

A_1:	constant, Kerner–Lewis equation [eq. (3)]
B_1, B_2:	constants, Kerner–Lewis equation [eqs. (3) and (4)]
E_c, E_f, E_m:	composite, filler, and matrix modulus [eqs. (3) and (4)]
E_{0c}, E_{0m}:	initial modulus of composite and of matrix (at $\epsilon \sim 0$)
E_p:	initial modulus determined from "load–unload" test
E_{sc}, E_{sm}:	secant modulus of composite and matrix
ϵ, ϵ_T:	axial and transverse strain
ϵ_0, ϵ_y:	elastic strain and yield strain
ϵ_p:	prestrain
Δl:	displacement recorded by extensometer
ϕ:	filler volume fraction
ϕ_m:	maximum packing fraction [eq. (5)]
ν, ν_{0m}, ν_{0c}:	Poisson ratio and initial Poisson ratio of matrix and of composite
σ, σ_0, σ_s, σ_y:	applied stress, elastic stress, calculated stress at $\epsilon = 7.5\%$ [eq. (6)] and yield stress
ζ:	volume strain

REFERENCES

1. P. H. T. Vollenberg, D. Heikens, and H. C. B. Ladan, *Polym. Compos,* **9,** 382 (1988).
2. I. Naqui and I. M. Robinson, *J. Mater. Sci.,* **28,** 1421 (1993).
3. C. B. Bucknall, *Nat. Phys. Sci.,* **231,** 31 (1971).
4. B. Pukánszky, M. Van Es, F. H. J. Marer, and G. Vörös, *J. Mater. Sci.,* **29,** 2350 (1994).
5. E. A. A. Van Hartingsveldt, Ph. D. Thesis, Technical University of Delft, The Netherlands (1987).
6. D. Heikens, S. D. Sjoerdsma, and W. J. Coumans, *J. Mater. Sci.,* **16,** 429 (1981).
7. A. Meddad and B. Fisa, to appear.
8. T. Mariyama, *Polym. Eng. Sci.,* **33,** 1494 (1993).
9. L. E. Nielsen and R. F. Landel, *Mechanical Properties of Polymers and Composites,* Marcel Dekker, Inc., New York, 1994.
10. S. Ahmed and F. R. Jones, *Composites,* **19,** 4933 (1988).
11. R. P. Hegler, G. Mennigard, and G. Vulpius, *Intern. Polym. Process,* **2,** 63 (1987).
12. L. Sinien, Y. Lin, Z. Xiaoguang, and Q. Zongneng, *J. Mater. Sci.,* **27,** 4633 (1992).
13. R. H. Beck, S. Matsuo, S. Newmann, and K. C. Rush, *J. Polym. Sci.,* **6,** 707 (1968).
14. T. S. Chow, *J. Polym. Sci.,* **16,** 967 (1978).